Food Bioprocess Technol (2011) 4:1357–1366
DOI 10.1007/s11947-009-0222-y

ORIGINAL PAPER

Application of Image Analysis and Artificial Neural Network to Predict Mass Transfer Kinetics and Color Changes of Osmotically Dehydrated Kiwifruit

Milad Fathi · Mohebbat Mohebbi · Seyed Mohammad Ali Razavi

Received: 6 March 2009 / Accepted: 9 June 2009 / Published online: 4 July 2009

Abstract The objectives of this study were to use image analysis and artificial neural network to predict mass transfer kinetics and color changes of osmotically dehydrated kiwifruit slices. Kiwifruits were dehydrated implementing four different sucrose concentrations, at three processing temperatures and during four osmotic time periods. A multilayer neural network was developed by using the operation conditions as inputs to estimate water loss, solid gain, and color changes. It was found that artificial neural network with 16 neurons in hidden layer gives the best fitting with the experimental data, which made it possible to predict solid gain, water loss, and color changes with acceptable mean-squared errors (1.005, 2.312, and 2.137, respectively). These results show that artificial neural network could potentially be used to estimate mass transfer kinetics and color changes of dehydrated kiwifruit.

Keywords Artificial neural network · Image analysis · Kiwifruit · Osmotic dehydration

Introduction

Kiwifruit (*Actinidia deliciosa*) is a highly nutritional fruit due to its high level of vitamin C and its strong antioxidant capacity because of a wide number of phytonutrients including carotenoids, lutein, phenolics, flavonoids, and chlorophyll (Cassano et al. 2006). Furthermore, kiwifruit has a very short shelf-life due to high moisture content (above 80% by weight), and it is necessary to use various preservation methods to increase its shelf life.

Osmotic dehydration is used as a pre-treatment to many preservation processes such as freezing, freeze drying, microwave drying, and air drying to improve nutritional, sensorial, and functional properties of fruits without changing their integrity. This operation is used for the partial removal of water from plant tissues by immersion in a hypertonic (osmotic) solution. Water removal is based on the natural and nondestructive phenomenon of osmosis across cell membranes. The diffusion of water out of the plant's tissues is accompanied by the simultaneous counter diffusion of solutes from the osmotic solution into the tissue. There may also be minor flow of other solutes from fruit to solution (Sun 2005). The existence of those simultaneous and opposite mass transfers is one of the main difficulties in modeling osmotic dehydration kinetics (solid gain and water loss) of fruits (Spiazzi and Mascheroni 1997). However, there are several models reported in the literature for the estimation of mass transfer kinetic during osmotic dehydration, mostly based on the solution of Fick's second law (El-Aouar et al. 2003; Garcia et al. 2007; Rastogi and Niranjan 1998) or nonlinear regression (Nieuwenhuijzen et al. 2001). Although these models give a reasonable fitting of the experimental data, their application is limited due to their semiempirical nature, and therefore, they are only capable of estimating data within the processing conditions for which they were developed or they depend on a large number of physical properties of fruits (Ochoa-Martínez et al. 2007).

Artificial neural networks (ANNs) are powerful modeling techniques that exhibit analogies to the way arrays of neurons function in biological learning and memory. ANNs offer several advantages over conventional modeling techniques because they can model based on no assumptions concerning the nature of the phenomenological mechanisms and

M. Fathi · M. Mohebbi (✉) · S. M. A. Razavi
Department of Food Science and Technology,
Ferdowsi University of Mashhad,
P.O. Box 91775-1163, Mashhad, Iran
e-mail: mohebbat2000@yahoo.com

understanding the mathematical background of problem underlying the process and the ability to learn linear and nonlinear relationships between variables directly from a set of examples. The fundamental building blocks of ANN are units called nodes (neurons) comparable to biological neurons and weighted connections that can be likened to synapses in biological systems. Nodes are simple information processing elements (Haykin 1994; Vinod and Vikrant 2002; Amin et al. 2009).

Some researchers have used ANN as a useful modeling tool to predict some physical characteristics of dried or dehydrated products. Poligné et al. (2002) introduced the application of ANN during a dehydration–impregnation–soaking process of pork meat. They constructed an ANN by using smoke flavoring concentration, temperature, and sugar concentration as input vectors to predict mass transfer kinetic and quality changes of pork meat. Ochoa-Martínez and Ayala-Apaonte (2007) developed an ANN model for prediction of mass transfer kinetics during osmotic dehydration of apple. They used temperature and concentration of osmotic solution, immersion time, surface area, solution to fruit mass ratio, and agitation level as the input variables to estimate solid gain and water loss of dehydrated apple. The authors developed an ANN which included one hidden layer and four hidden neurons. The developed ANN was better performed compared to the corresponding linear multivariable regression. Amiryusefi and Mohebbi (2008) employed feedforward neural network to estimate the solid gain, water loss as well as moisture content (w.b.) of dehydrated potato. Their results showed that the best ANN, which was developed based on two hidden layers and ten neurons per each hidden layer, is capable to predict these parameters with the correlation coefficients more than 0.98 in all cases.

In addition to mass transfer kinetics, the color of the dehydrated product is an important quality factor, which is affected by the operation conditions. Color usually is the first quality parameter that is evaluated by consumers and is critical in the acceptance of the product. Recently, image analysis has been used as a promising approach to the objective assessment of a dried product's quality. Riva et al. (2005) investigated the influence of osmotic agents (sucrose and sorbitol solutions) and syrup composition on chemical–physical properties, structure collapse, and color changes of osmo-air-dehydrated apricot cubes. They reported color parameters showing a slight change after the osmotic step: a^* and b^* components maintained their initial values (no browning), whereas L^* values diminished (darkening). These authors also mentioned that using sorbitol as the osmotic solution led to the highest protective effect on the color of dried apricot compared to the other tested solution. Mohebbi et al. (2007) investigated the possibility of machine vision and ANN application for prediction of moisture content (w.b.) of dried shrimp. They considered six color parameters of dried shrimp as inputs of ANN and found that the optimum configuration, which included five neurons per hidden layer, could predict moisture content (w.b.) of dried shrimp with coefficient of determination of 0.86. These researchers stated that application of image processing in conjunction with ANN could reduce processing time and cost by minimizing chemical experiments such as determination of moisture content.

This study aimed to investigate the dependence of mass transfer kinetics (water loss (WL) and solid gain (SG)) as well as color changes of dehydrated kiwifruit on different osmotic conditions (concentration, temperature, and duration of osmotic process) and study the efficiency of ANN for predicting these parameters.

Materials and Methods

Preparation of Samples

Kiwifruits, cultivar Hayward, were purchased in Sari, Iran and stored at 1 °C before used in the experiments. Initial moisture and soluble solid content were 84.5±0.9 (% w.b.) and 12.4±0.7° Brix, respectively. Kiwifruits were cut into 40 mm diameter and 10 mm thickness slices.

Osmotic Dehydration and Mass Transfer Kinetic Analysis

Kiwifruit slices were weighed and placed into a beaker which contained osmotic solutions prepared with food grade sucrose. Kiwifruits were dehydrated with four different sugar concentrations (30, 40, 50, and 60° Brix) at temperatures of 20, 40 and 60 °C. A fruit/solution ratio of 1:10 by weight was used to avoid an excessive dilution of osmotic solution. Osmotic dehydration was performed under the same magnetic agitation to maintain uniform temperature and concentration throughout the experiment. Immersion times of 0.5, 1, 1.5, and 2 h were tested. At the end of the osmotic dehydration process, samples were taken out of the sucrose solution, washed with distilled water to remove the adhered osmotic solution, and blotted with adsorbent paper. The weight (by means of an electronic balance reading with an accuracy of 0.01 g; AND EK-300*i*, Japan) and moisture content (percent w.b.; at 90 °C until constant weight was obtained) were measured individually. The experiments were conducted as a 4×3×4 factorial design (4 osmotic concentrations × 3 osmotic temperatures × 4 osmotic times) with four replications.

Two quantities represent adequately the osmotic dehydration process: The WL and SG were calculated based on the following equations (Giangiacomo et al. 1987; Shi et al. 2009):

$$WL = \frac{(WW_0) - (W_t - WS_t)}{(WS_0 + WW_0)} \times 100 \quad (1)$$

$$SG = \frac{(WS_t - WS_0)}{(WS_0 + WW_0)} \times 100 \quad (2)$$

where WW_0 is the weight of water and WS_0 is the weight of solids initially present in the kiwifruit. W_t and WS_t are the weight of the kiwifruit and the weight of the solids after osmotic dehydration, respectively.

Image Acquisition and Analysis

In order to investigate the effect of osmotic dehydration on color changes of dehydrated kiwifruit samples, the following procedure was applied:

(a) A computer vision system generally consists of four basic components: illumination, a camera, computer hardware, and software. In this research, sample illumination was achieved with three fluorescent lights (Opple, 8 W, model: MX396-Y82; 60 cm in length) with a color index (Ra) close to 95%. The illuminating lights were placed in a wooden box, 45 cm above the sample and at the angle of 45º with sample plane to give a uniform light intensity over the kiwifruit sample (Quevedo et al. 2009). The interior walls of the wooden box were painted black to minimize background light. A color digital camera (Canon Powershot, Model A520, Japan) with 4 Mega pixels of resolution was located vertically at a distance of 25 cm from the sample. The angle between the camera lens axis and lightening sources was around 45º. The iris was operated in manual mode, with the lens aperture of 4 and speed 1/10 s (no zoom, no flash) to achieve high uniformity and repeatability. Images were captured with the mentioned digital camera at 2,272×1,704 pixels and connected to the USB port of Pentium IV, 2.4 GHz computer. Canon Digital Camera Solution Software (version 22) was used to acquire the images in the computer in JPEG format.

(b) Image preprocessing: In order to improve background's contrast of digital images, preprocessing was accomplished using Adobe Photoshop (Adobe, v.7.0).

(c) Segmentation: Image segmentation was performed to separate the true image of the kiwifruit sample from background, using threshold combined with an edge detection approach based on the Laplacian-of-Gaussian filter (Castleman 1996).

(d) Conversion of RGB chromatic space into $L^*a^*b^*$ units: Since the computer vision system perceived color as RGB signals, which is device-dependent (Fernández et al. 2005), the images taken were converted into $L^*a^*b^*$ units to ensure color reproducibility. In the $L^*a^*b^*$ space, the color perception is uniform, and therefore, the Euclidean distance between two colors corresponds approximately to the color difference perceived by the human eye (Pedreschi et al. 2007). Transformation RGB into L^*a^*b space was performed according to a direct model similar to the procedure described by León et al. (2006).

The color changes (ΔE) of dehydrated kiwifruits were estimated from the coordinates of color by applying the following equation (Shafafi Zenoozian et al. 2008):

$$\Delta E = \left[(L^*_2 - L^*_1)^2 + (a^*_2 - a^*_1)^2 + (b^*_2 - b^*_1)^2\right]^{\frac{1}{2}} \quad (3)$$

where L^* is lightness component, which ranges from 0 to 100 and parameter a^* (from green to red) and b^* (from blue to yellow) are two chromatic components, which range from −120 to 120. Subscripts 1 and 2 are referred to as color components before and after osmotic dehydration, respectively. In this study, the image analysis was performed using Imagj software version 1.40g.

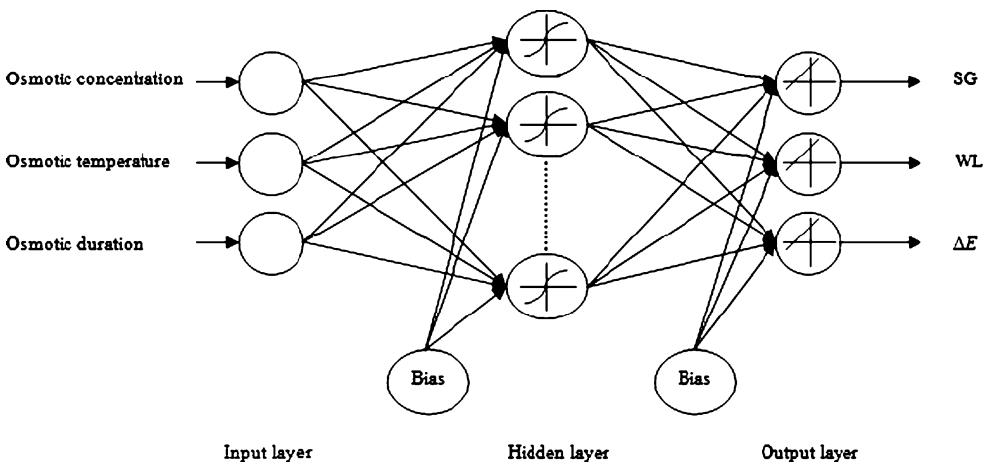

Fig. 1 Multilayer feedforward neural network architecture with one hidden layer for prediction solid gain, water loss, and ΔE of osmotically dehydrated kiwifruit

Artificial Neural Network

In this study, fully interconnected multilayer feedforward network, which is the most widely used ANN, was applied for modeling mass transfer kinetics and color changes of osmotically dehydrated kiwifruit. One of the commonly used feedforward ANN architectures is multilayer perceptron (MLP) network. The main advantages of MLP compared to other neural model structures are that it is easy to implement and it can approximate any input/output map (Menhaj 1998). MLP consists of (a) an input layer with neurons representing input variables to the problem, (b) an output layer with neuron(s) representing the dependent variable(s), and (c) one or more hidden layers containing neuron(s) to help capture the nonlinearity in the system (Fig. 1). The complexity of the MLP network depends on the number of layers and the number of neurons in each layer. The hidden layer maps the input pattern x with output pattern y through a series of interconnected weights. Mathematically (Razavi et al. 2003):

$$y_j = \sum_{i=1}^{n} f\left(w_{ij}x_i\right) + b_j \tag{4}$$

where W_{ij} is the weight of the ith input vector that is connected to the jth neuron; n is number of inputs to the neuron; b_j is the bias associated with the jth neuron, which adds a constant term in the weighted sum to improve convergence; and f is the activation function that determines the processing inside the neuron. Activation function can be linear or nonlinear (commonly hyperbolic tangent or sigmoid) function depending on the network topology. In this work, the operational variables of osmotic process of kiwifruit (concentration, temperature of osmotic solution, and osmotic duration) were used as inputs, and solid gain, water loss, and ΔE were considered as outputs. A hyperbolic tangent activation function (Eq. 5) was chosen to be used in the hidden layer, due to lower calculated mean-squared error values than the respective sigmoid function, while a linear function was used in the output layer.

$$\tanh = \frac{e^{x} - e^{-x}}{e^{x} + e^{-x}} \tag{5}$$

Two important factors must be considered in order to ensure a successful modeling of MLP. First, is the number of hidden layers and second is the number of neurons in each hidden layer. Since almost all of the problems in neural network modeling could be solved with one hidden layer (Chen et al. 2001; Kashaninejad et al. 2008; Mohebbi et al. 2007; Movagharnejad and Nikzad 2007; Ochoa-Martínez and Ayala-Apaonte 2007; Mitra et al. 2009), an ANN with three layers was used in this research. In addition, using too many hidden layers may lead to problem of data overfitting, affecting the system's generalization capability (Abdullah et al. 2006). On the other hand, to find the best architecture, different networks were built with different hidden neurons varying from 2 to 20.

In total, 192 data were collected for the four different concentrations and osmotic times and three osmotic temperatures. First, the data order was randomized and then the data were divided into three partitions. The first partition (training data) was used to perform the training of the network (40% of data). The second one (cross-validation data) was used to evaluate the prediction quality of the network during the training (30% of data). For the purpose of estimating the performance of the trained network on new data, a third partition, which never was seen by the artificial neural network during the training and cross-validation process, was used (30% of data) for testing. During training, momentum value was fixed at 0.7, and learning rate was determined at level 1 on the hidden layer and 0.1 at the output layer. The training process was carried on for 1,000 epochs or until the cross-validation data's mean-squared error (MSE), calculated by Eq. 6, did not improve for 100 epochs to avoid over-fitting of the network.

Backpropagation algorithm was used to implement supervised training of the network. Backpropagation is based on searching an error surface (error as a function of ANN weights) using gradient descent for point(s) with minimum error. Each iteration in backpropagation constitutes two sweeps: forward activation to produce a solution, and the backwards propagation of the computed error to modify the neurons' weights (Movagharnejad and Nikzad 2007).

Testing was carried out with the best weights stored during the training. Evaluation of the performance of the trained network was based on the accuracy of the network in the test partition. Therefore, MSE, normalized mean-squared error (NMSE), mean absolute error (MAE), and correlation coefficient (R) for each output were calculated by using Eqs. 6–10 (Mohebbi et al. 2008) based on testing data and were used to compare the performance of different ANN architectures. In this study, the ANN models were constructed by Neuro-solution for Excel software release 5.0, produced by NeuroDimension, Inc.

$$\mathrm{MSE} = \frac{\sum_{i=1}^{N} (O_i - T_i)^2}{N} \tag{6}$$

$$\mathrm{NMSE} = \frac{1}{\sigma^2}\frac{1}{N}\sum_{i=1}^{N} (O_i - T_i)^2 \tag{7}$$

Table 1 Means and standard deviations of SG, WL, WL/SG ratio, and ΔE during osmotic dehydration of kiwifruit at different concentrations (C), temperatures (T), and immersion times (h)

C (%)	T (ºC)	SG (%)				WL (%)				WL/SG ratio				ΔE			
		0.5h	1h	1.5h	2h	0.5h	1h	1.5h	2h	0.5h	1h	1.5h	2h	0.5h	1h	1.5h	2h
30	20	1.03±0.6	1.22±0.7	1.67±0.5	2.07±0.3	7.52±0.8	7.58±1.1	8.57±1.2	10.63±0.5	7.30±2.1	6.23±0.94	5.15±2.1	5.15±0.7	1.89±0.09	2.30±0.11	2.19±0.08	3.19±0.13
30	40	1.95±0.6	2.68±0.6	2.79±0.2	3.68±0.4	10.09±0.9	12.99±0.9	16.32±1.7	17.00±0.8	5.18±1.29	4.85±0.99	5.84±0.82	4.62±0.35	5.20±0.21	2.47±0.18	2.31±0.15	3.42±0.11
30	60	3.41±0.8	5.36±0.5	6.76±1.2	7.38±0.8	17.32±0.6	21.37±0.7	23.53±2	26.52±1.7	5.08±1.07	3.99±0.47	3.48±0.49	3.59±0.55	9.25±0.17	8.02±0.18	9.12 0.31	8.39±0.29
40	20	1.38±0.3	1.52±0.6	2.04±0.7	4.11±1.3	9.36±0.6	10.65±1.3	12.24±0.4	13.83±1.5	6.77±0.53	7.01±3.98	6.00±2.39	3.36±0.94	2.02±0.14	2.25±0.26	2.98±0.31	3.14±0.26
40	40	2.20±0.3	2.84±0.6	3.16±0.3	5.76±1.1	15.56±1.3	19.25±0.8	23.30±0.6	27.97±1.2	7.07±1.31	6.78±0.71	7.37±0.99	4.86±0.82	2.65±0.21	3.14±0.48	3.20±0.63	4.43±0.37
40	60	3.80±0.4	5.48±1.1	7.82±1.2	8.94±1.4	22.18±0.7	27.72±0.5	34.37±0.8	37.94±1.2	5.84±0.67	5.06±1.3	4.40±0.7	4.24±0.79	8.83±0.49	6.02±0.5	5.34±0.62	9.73±0.4
50	20	2.28±0.4	2.42±0.4	3.17±0.3	4.90±0.5	9.89±0.4	15.75±1.3	15.49±0.5	18.17±1.1	4.34±1.55	6.50±0.26	4.89±1.9	3.71±1.55	0.92±0.11	2.40±0.22	3.17±0.18	2.61±0.29
50	40	3.07±0.3	4.20±0.9	5.16±0.6	5.95±1.2	15.49±0.4	23.40±0.7	29.71±0.8	31.75±0.7	5.05±0.48	5.57±0.46	5.76±1.72	5.34±1.14	1.82±0.31	2.16±0.37	3.79±0.27	4.04±0.62
50	60	4.34±0.3	6.25±0.2	8.27±0.6	9.02±1.1	23.18±0.4	33.22±1	42.22±1.4	45.68±0.3	5.35±0.82	5.31±0.07	5.11±1.89	5.06±1.19	8.20±0.46	6.70±0.71	7.74±0.53	6.82±0.58
60	20	2.57±1	2.69±1	3.83±1.7	4.92±1.9	13.80±0.7	18.31±0.6	19.60±1.9	19.80±1.7	5.36±1.3	6.81±2.07	5.12±2.21	4.02±2.49	2.99±0.39	1.66±0.17	2.49±0.53	2.05±0.15
60	40	4.08±1.2	4.25±0.8	6.18±1.2	6.19±0.5	18.32±1.7	26.01±1.2	33.83±1.2	37.82±0.3	4.49±1.35	6.12±2.46	5.47±1.25	6.11±2.74	3.81±0.48	2.65±0.27	4.96±0.78	4.65±0.27
60	60	6.28±0.9	6.89±0.4	8.38±0.8	9.28±0.5	32.63±0.9	40.82±0.7	46.95±1.5	52.98±0.4	5.20±0.67	5.92±0.43	5.60±0.95	5.71±1.52	6.06±0.28	5.86±0.41	8.03±0.45	10.09±0.53

Table 2 Means and standard deviations of the changes of the chromatic parameters (L^*, a^*, and b^*) during osmotic dehydration of kiwifruit at different concentrations (C), temperatures (T), and immersion times (h)

C (%)	T (°C)	$L^*_2-L^*_1$				$a^*_2-a^*_1$				$b^*_2-b^*_1$			
		0.5h	1h	1.5h	2h	0.5h	1h	1.5h	2h	0.5h	1h	1.5h	2h
30	20	1.58±0.04	0.20±0.01	1.89±0.21	2.52±0.24	−0.40±0.05	−0.62±0.06	−0.18±0.04	−0.44±0.05	0.37±0.02	0.84±0.07	0.64±0.07	1.76±0.09
30	40	1.74±0.09	2.02±0.31	1.68±0.1	2.97±0.08	−0.41±0.06	0.21±0.02	1.07±0.09	1.38±0.14	0.27±0.03	1.23±0.06	−0.46±0.04	0.43±0.05
30	60	0.93±0.07	0.48±0.08	−0.08±0.01	1.60±0.06	7.61±0.21	6.56±0.38	8.07±0.32	7.41±0.43	−4.96±0.09	−4.23±0.12	−3.41±0.15	−3.31±0.43
40	20	1.08±0.09	1.12±0.27	2.53±0.16	2.74±0.19	−0.35±0.03	−0.14±0.02	−0.37±0.04	0.21±0.03	0.63±0.02	−0.20±0.01	1.25±0.02	0.78±0.6
40	40	2.15±0.18	2.29±0.45	2.42±0.04	3.37±0.48	0.61±0.04	−0.17±0.02	−0.63±0.05	2.55±0.09	0.70±0.02	1.13±0.08	1.55±0.27	−0.16±0.05
40	60	1.45±0.07	0.58±0.03	1.81±0.05	3.04±0.2	7.55±0.08	5.27±0.37	4.89±0.31	9.17±0.61	−4.19±0.33	−2.70±0.19	−0.15±0.01	−0.94±0.01
50	20	0.57±0.07	1.00±0.11	2.75±0.22	1.43±0.18	0.50±0.02	−0.13±0.03	1.13±0.16	0.21±0.04	0.07±0.01	0.85±0.02	−0.19±0.02	1.01±0.03
50	40	1.10±0.09	0.90±0.03	2.11±0.31	3.22±0.02	−0.42±0.03	0.08±0.02	0.88±0.02	0.07±0.01	1.39±0.25	1.59±0.32	2.48±0.48	2.12±0.09
50	60	1.33±0.08	1.30±0.12	2.75±0.27	3.42±0.33	6.47±0.21	6.39±0.51	7.04±0.66	5.39±0.72	−3.99±0.17	−1.15±0.08	−0.76±0.03	−0.90±0.02
60	20	1.88±0.19	0.57±0.1	2.05±0.21	1.36±0.16	−0.97±0.04	0.15±0.02	0.53±0.03	0.22±0.04	1.46±0.08	−0.47±0.04	0.04±0.01	−0.11±0.01
60	40	2.10±0.37	1.76±0.13	4.58±0.28	4.27±0.09	−0.36±0.01	0.10±0.01	0.38±0.02	0.43±0.01	2.65±0.09	1.67±0.05	1.20±0.06	1.33±0.09
60	60	2.42±0.13	2.15±0.18	2.93±0.17	2.72±0.25	5.21±0.05	5.08±0.06	7.20±0.08	9.49±0.09	−1.62±0.05	−1.03±0.19	−0.84±0.03	−1.16±0.07

Table 3 Successive mean squares from the analysis of variance of the solid gain, water loss, color changes, and changes of three chromatic parameters (L^*, a^*, and b^*)

Source	Degree of freedom	Mean square					
		SG	WL	ΔE	$L^*_2-L^*_1$	$a^*_2-a^*_1$	$b^*_2-b^*_1$
A	3	42.07**	1,974.6**	3.18*	0.55 ^{NS}	31.75 ^{NS}	0.98 ^{NS}
B	2	280.53**	6,307.66**	520.15**	0.54 ^{NS}	34.87**	0.43 ^{NS}
C	3	81.78**	1,319.47**	16.12**	1.54 ^{NS}	0.87*	0.95 ^{NS}
$A\times B$	6	0.502 ^{NS}	102.25**	3.28*	0.03 ^{NS}	1.08 ^{NS}	0.12 ^{NS}
$A\times C$	9	1.74*	47.41**	4.34*	0.76 ^{NS}	1.27 ^{NS}	0.31 ^{NS}
$B\times C$	6	5.15**	115.45**	2.75*	0.47 ^{NS}	1.13 ^{NS}	0.19 ^{NS}
$A\times B\times C$	18	0.54 ^{NS}	7.43**	4.79*	0.09 ^{NS}	0.14 ^{NS}	0.04 ^{NS}
Error	144	1.22	1.33	1.9	1.11	1.21	1.18 ^{NS}
Total	191						

A osmotic concentration, *B* osmotic temperature, *C* osmotic time, *NS* not significant

**p=0.001; *p=0.05

$$\mathrm{MAE} = \frac{1}{N}\sum_{i=1}^{N}|O_i - T_i| \tag{8}$$

$$R = \sqrt{1 - \frac{\sum_{i=1}^{N}[O_i - T_i]^2}{\sum_{i=1}^{N}[O_i - T_m]^2}} \tag{9}$$

where O_i is the ith actual value, T_i is the ith predicted value, N is the number of data, σ^2 is the variance, and

$$T_m = \frac{\sum_{i=1}^{N} O_i}{N}. \tag{10}$$

Statistical Analysis

Analysis of variance (ANOVA) of data was performed using a computerized statistical program called "MSTAT" version C, and determination of significant differences of means was carried out by "Duncan" test at 1% significant level using the above software program.

Results and Discussion

Effect of Osmotic Dehydration on Mass Transfer Kinetics and Color Changes

Average values of solid gain, water loss, water loss/solid gain ratio, color changes, and changes of each chromatic parameter during the osmotic dehydration of kiwifruit slices for the whole treatments are presented in Tables 1 and 2, respectively. In Table 3, parts of ANOVA tables for solid

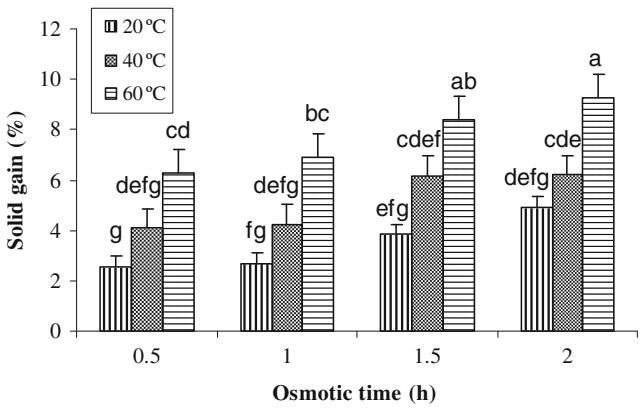

Fig. 2 Effect of osmotic temperature and duration for concentration of 60% on solid gain of osmotically dehydrated kiwifruit

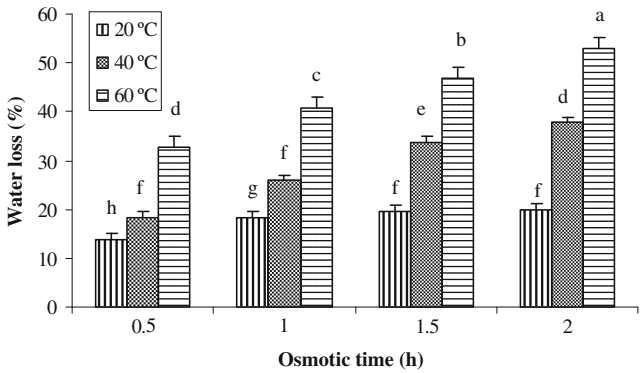

Fig. 3 Effect of osmotic temperature and duration for concentration of 60% on water loss of osmotically dehydrated kiwifruit

Table 4 Errors in prediction of solid gain, water loss, and ΔE using ANN with different number of neurons in single hidden layer for osmotically dehydrated kiwifruit

No. of neurons	Solid gain			Water loss			ΔE		
	MSE	NMSE	MAE	MSE	NMSE	MAE	MSE	NMSE	MAE
2	3.042	0.515	1.363	79.02	0.536	7.37	8.37	1.058	2.215
3	1.109	0.175	0.791	12.864	0.091	2.833	2.494	0.317	1.299
4	1.078	0.174	0.796	6.000	0.038	1.991	2.279	0.273	4.473
5	1.450	0.251	0.914	8.775	0.079	2.226	2.199	0.292	1.174
6	1.727	0.285	1.003	7.934	0.058	2.11	2.606	0.339	1.222
7	1.336	0.274	0.882	5.261	0.058	1.887	3.076	0.413	1.417
8	1.552	0.206	0.963	5.311	0.039	1.846	3.339	0.536	5.642
9	1.069	0.235	0.786	6.638	0.051	2.032	3.504	0.458	1.365
10	1.322	0.181	0.868	2.995	0.018	1.303	4.001	0.432	1.519
11	1.075	0.174	0.814	2.553	0.017	1.164	3.022	0.412	1.176
12	1.513	0.209	0.954	3.492	0.028	1.366	3.392	0.384	5.241
13	1.174	0.214	0.733	2.546	0.017	1.302	2.398	0.298	4.022
14	1.124	0.218	0.776	3.866	0.033	1.574	2.145	0.429	1.19
15	1.527	0.213	0.893	5.394	0.039	1.832	2.91	0.356	4.375
16	1.005	0.16	0.798	2.312	0.039	1.848	2.137	0.272	1.168
17	1.267	0.175	0.877	3.709	0.030	1.493	3.673	0.51	1.451
18	1.343	0.209	0.852	3.757	0.030	1.559	3.018	0.397	1.302
19	1.505	0.264	0.904	6.761	0.052	1.898	3.905	0.418	1.448
20	1.314	0.244	0.876	2.419	0.023	1.283	2.717	0.434	1.256

gain, water loss, color changes, and changes of each chromatic parameter are given. It was found that solid gain and water loss increased significantly as temperature, concentration, and osmotic duration increased. Therefore, samples immersed in osmotic solution of 60% at 60 ºC for 2 h had the greatest solid gain (9.28%) and water loss (52.98%). The solid gain and water loss at the end of the osmotic process for the four levels of immersion times and three osmotic temperatures for the

Table 5 Corresponding weight and bias values of each neuron for optimum ANN configuration used to predict SG, WL, and ΔE of osmotically dehydrated kiwifruit

Hidden neurons	Bias	Input neurons			Output neurons		
		Concentration	Temperature	Time	Solid gain	Water loss	ΔE
1	0.76968	0.03497	−1.20001	−0.18476	−0.35974	−0.29263	−0.18091
2	0.47119	−0.32792	−0.37287	−0.68928	0.25142	0.059	0.27054
3	0.14329	0.32552	−0.48708	−0.08214	−0.3209	−0.21015	−0.34749
4	0.48321	0.00897	−0.94081	0.08359	−0.20761	0.11877	0.35841
5	0.19503	0.30375	0.46528	0.1889	−0.06018	0.07583	−0.08675
6	0.33798	−0.05073	0.15364	0.26056	0.23057	0.04786	−0.13814
7	−0.52286	0.57002	0.06464	−0.00985	−0.1575	−0.29013	−0.31561
8	−0.00388	0.54773	−0.4758	0.1785	−0.03775	0.28899	0.20374
9	−0.38034	−0.81863	−0.04547	−0.40282	0.01505	0.02413	0.42987
10	0.24197	−0.47857	0.04043	−0.40559	−0.19982	0.37225	−0.01796
11	−0.44819	0.39526	0.52965	0.39421	−0.05423	−0.02367	−0.31778
12	−0.35041	0.22844	−0.32133	−0.41326	−0.15015	−0.14233	−0.41029
13	−0.25663	0.44577	0.41055	0.19203	0.30183	0.26501	0.1056
14	0.27025	0.3265	0.0028	0.42678	0.16696	0.39431	−0.29234
15	−0.0671	−0.10848	−0.06417	0.27949	−0.19963	0.19242	−0.21289
16	0.26917	−0.02665	0.39768	−0.27706	−0.04674	−0.11674	−0.14285
Bias					−0.26384	0.2384	0.10634

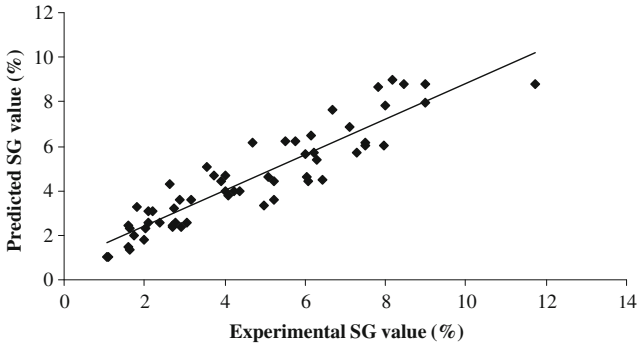

Fig. 4 Experimental vs. predicted values for solid gain of osmotically dehydrated kiwifruit by optimum ANN configuration (R=0.92)

concentration of 60% are shown in Figs. 2 and 3, respectively. The same tendencies were also found for the osmotic concentrations of 30%, 40%, and 50%. Increasing WL and SG by increasing temperature could be attributed to the effect of temperature on the membrane permeability by making it more permeable to water and sugar exchanges. On the other hand, by increasing sucrose concentration, the osmotic pressure in the kiwifruit tissue is increased, which led to increase water loss and solid gain.

The effect of operating conditions can also be assessed by water loss/solid gain ratio. In an osmotic dehydration process, the higher water loss is more favorable than solid gain. On the other hand, high solid gain affects negatively the quality and sensory characteristics of the dehydrated fruit. When high levels of sugar are infiltrated into the fruit during osmotic dehydration, significant sensory alterations can occur, and the osmotically dehydrated product may present a different taste from the fresh fruit (Rodrigues and Fernandes 2007). The kiwifruit samples, treated with osmotic solution of 40% at 40 °C for 1.5 h, had the greatest water loss/solid gain ratio (average value of 7.37).

As Table 2 shows, the variations in ΔE and b^* are statistically significant, whereas the relationship between chromatic parameters L^* and b^* and operation conditions were not statistically significant.

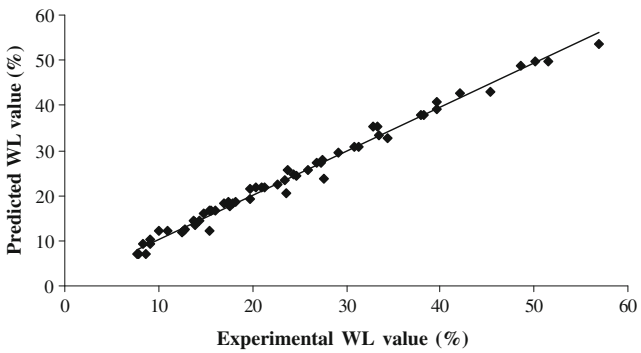

Fig. 5 Experimental vs. predicted values for water loss of osmotically dehydrated kiwifruit by optimum ANN configuration (R=0.994)

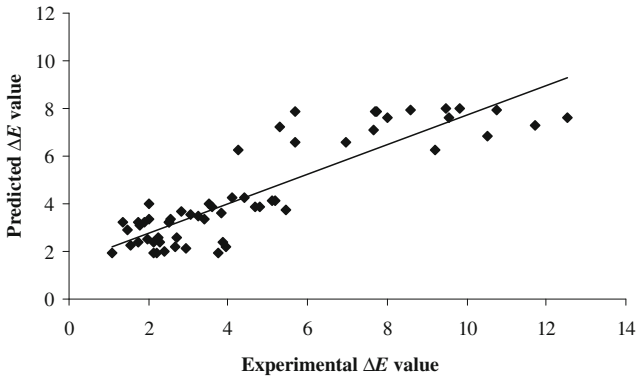

Fig. 6 Experimental vs. predicted values for ΔE of osmotically dehydrated kiwifruit by optimum ANN configuration (R=0.88)

Table 1 reveals that increasing temperature caused an increase in ΔE values. The chromatic parameter a^* is found to be the major component that contributes most to the overall color change during osmotic dehydration of the kiwifruit. The a^* values increased significantly by increasing osmotic temperature, which shows diminishing of green color of dehydrated kiwifruits. This phenomenon can be attributed to the decay in chlorophyll pigments, which can be explained with Arrhenius-type temperature dependence of chlorophyll degradation (Nisha et al. 2004) or increased loss of liberated coloring compounds by migration into the solution (Tijskens et al. 2001). The samples were osmosed in osmotic solution of 60% at 60 ºC for 2 h subjected to the greatest color changes (average ΔE value of 10.09). Tijskens et al. (2001) found a similar trend during blanching of broccoli and green beans. Therdthai and Zhou (2009) reported that using a high temperature during drying of mint leaves could lead to conversion of chlorophylls to pheophytins, which caused to increase both a^* and ΔE values.

Artificial Neural Network Optimization

The optimum number of neurons in the hidden layer is determined by trial/error procedure based on minimizing the difference between estimated ANN outputs and experimental values. The error measures for estimation of solid gain, water loss, and ΔE during the testing process of different architectures of ANN with two to 20 neurons in the hidden layer are shown in Table 4. It was found that ANN with 16 hidden neurons had the minimum MSE values for solid gain (1.005), water loss (2.312), and ΔE (2.137) predictions. This architecture also had the lowest NMSE (0.16) as well as NMSE (0.272) and MAE (1.168) in the case of solid gain and ΔE estimation, respectively, and therefore, this one was chosen as the best ANN. Table 5 tabulates the weight and bias values of the chosen ANN, which could be used to predict mass transfer kinetics

and color changes of osmotically dehydrated kiwifruit slices under specific experimental conditions.

Artificial Neural Network Performance

The prediction efficiency of the chosen ANN model for testing data is presented in Figs. 4, 5, and 6 for SG, WL and ΔE, respectively, in which the predicted values are plotted against their experimentally measured values for the best configuration ANN (16 neurons in the hidden layer). The calculated correlation coefficient values for estimation of SG, WL, and ΔE (0.92, 0.994, and 0.88, respectively) were acceptable and revealed good agreement between predicted and experimental values. Therefore, the configuration of ANN model including 16 neurons in the hidden layer is efficiently suggested for prediction of solid gain, water loss, and ΔE of osmotically dehydrated kiwifruit slices.

Conclusions

The following conclusions are drawn from the investigation on osmotic dehydration of kiwifruit and the possibility of application of image analysis and artificial neural network to predict mass transfer kinetics and color changes of osmotically dehydrated kiwifruit:

1. Solid gain and water loss increased significantly when osmotic temperature, concentration, and immersion time increased. The effect of temperature was pronounced more than the others.
2. It was noted that as the processing temperature was increased, this could lead to color changes (ΔE).
3. A multilayer feedforward neural network based on three inputs (operation conditions) and 16 neurons in the single hidden layer was found to be the best model for predicting solid gain, water loss, and ΔE (outputs), which showed minimum MSE (1.005, 2.312, and 2.137, respectively) and high R (0.92, 0.994, and 0.88, respectively) values.
4. It seems that application of both image analysis and artificial neural network can lead to an automated, objective, and rapid inspection as well as online state prediction and control of osmotic dehydration of kiwifruit.

Acknowledgment The authors are thankful to Mr. Ghazvini for his assistance during the experiment works.

References

Abdullah, M. Z., Mohamad-Saleh, J., Fathinul-Syahir, A. S., & Mohd-Azami, B. M. N. (2006). Discrimination and classification of fresh-cut starfruits (*Averrhoa carambola* L.) using automated machine vision system. *Journal of Food Engineering, 76*, 506–523.

Amin, M., Navaz H.K., Kehtarnavaz, N., & Dabiri D. (2009) A systematic approach for solving large-scale problems by neural network: Open refrigerated display cases and droplet evaporation problems. Food and Bioprocess Technology. doi: 10.1007/s11947-008-0167-6.

Amiryusefi MR, & Mohebbi M (2008) Artificial neural network modeling of osmotic dehydration mass transfer kinetics of potato. In: 18th National Congress on Food Science and Technology, 15–17 October 2008, Mashhad, Iran.

Cassano, A., Figoli, A., Tagarelli, A., Sindona, G., & Drioli, E. (2006). Integrated membrane process for the production of highly nutritional kiwifruit juice. *Desalination, 189*, 21–30.

Castleman, K. (1996). *Digital image processing* (p. 667). Englewood Cliffs: Prentice Hall.

Chen, C. R., Ramaswamy, H. S., & Alli, I. (2001). Prediction of quality changes during osmo-convective drying of blueberries using neural network models for process optimization. *Drying Technology, 19* (3), 507–523.

El-Aouar, Â. A., Azoubel, P. M., & Murr, F. E. X. (2003). Drying kinetics of fresh and osmotically pre-treated papaya (*Carica papaya* L.). *Journal of Food Engineering, 59*, 85–91.

Fernández, L., Castillero, C., & Aguilera, J. M. (2005). An application of image analysis to dehydration of apple discs. *Journal of Food Engineering, 67*, 185–193.

Garcia, C. C., Mauro, M. A., & Kimura, M. (2007). Kinetics of osmotic dehydration and air-drying of pumpkins (*Cucurbita moschata*). *Journal of Food Engineering, 82*, 284–291.

Giangiacomo, R., Torreggiani, D., & Abbo, E. (1987). Osmotic dehydration of food. Part I. Sugar exchange between fruit and extracting syrup. *Journal of Food Processing and Preservation, 11*, 183–195.

Haykin, S. (1994). *Neural network: A comprehensive foundation* (pp. 22–24). Canada: Prentice Hall.

Kashaninejad, M., Dehghani, A. A., & Kashiri, M. (2008). Modeling of wheat soaking using two artificial neural networks (MLP and RBF). *Journal of Food Engineering, 91*, 602–607.

León, K., Mery, D., Pedreschi, F., & León, J. (2006). Color measurement in L*a*b units from RGB digital images. *Food Research International, 39*, 1084–1091.

Menhaj, M. B. (1998). *Fundamentals of neural networks*. Tehran: Professor Hesabi.

Mitra P, Barman PC & Chang KS (2009) Coumarin extraction from *cuscuta reflexa* using supercritical fluid carbon dioxide and development of an artificial neural network model to predict the coumarin yield. Food and Bioprocess Technology. doi: 10.1007/s11947-008-0179-2.

Mohebbi M, Akbarzadeh Totonchi MR, Shahidi F & Poorshehabi MR (2007) Possibility evaluation of machine vision and artificial neural network application to estimate dried shrimp moisture. In: 4th Iranian Conference on Machine Vision, Image Processing and Application, 14–15 February 2007, Mashhad, Iran.

Mohebbi, A., Taheri, M., & Soltani, A. (2008). A neural network for predicting saturated liquid density using genetic algorithm for pure and mixed refrigerants. *International Journal of Refrigeration, 31*, 1317–1327.

Movagharnejad, K., & Nikzad, M. (2007). Modeling of tomato drying using artificial neural network. *Computers and Electronics in Agriculture, 59*, 78–85.

Nieuwenhuijzen, N. H. V., Zareifard, M. R., & Ramaswamy, H. S. (2001). Osmotic drying kinetics of cylindrical apple slices of different sizes. *Drying Technology, 19*(3 & 4), 525–545.

Nisha, P., Singhal, R. S., & Pandit, A. B. (2004). A study on the degradation kinetics of visual green colour in spinach *(Spinacea oleracea* L.) and the effect of salt therein. *Journal of Food Engineering, 64*, 135–142.

Ochoa-Martínez, C. I., & Ayala-Apaonte, A. A. (2007). Prediction of mass transfer kinetics during osmotic dehydration of apples using neural networks. *LWT, 40*, 638–645.

Ochoa-Martínez, C. I., Ramaswamy, H. S., & Ayala-Aponte, A. A. (2007). ANN-based models for moisture diffusivity coefficient and moisture loss at equilibrium in osmotic dehydration process. *Drying Technology, 25*(5), 775–783.

Pedreschi, F., León, J., Mery, D., Moyano, P., Pedreschi, R., Kaack, K., et al. (2007). Color development and acrylamide content of pre-dried potato chips. *Journal of Food Engineering, 79*, 786–793.

Poligné, I., Broyart, B., Trystram, G., & Collignan, A. (2002). Prediction of mass-transfer kinetics and product quality changes during a dehydration–impregnation soaking process using artificial neural networks. Application to pork curing. *Food Science and Technology-Lebensmittel-Wissenschaft & Technologie, 35*, 748–756.

Quevedo, R.A., Aguilera, J.M., & Pedreschi, F. (2009) Color of salmon fillets by computer vision and sensory panel. Food and Bioprocess Technology. doi: 10.1007/s11947-008-0106-6.

Rastogi, N. K., & Niranjan, K. (1998). Enhanced mass transfer during osmotic dehydration of high pressure treated pineapple. *Journal of Food Science, 63*, 508–511.

Razavi, S. M. A., Mousavi, S. M., & Mortazavi, S. A. (2003). Dynamic prediction of milk ultrafiltration performance: A neural network approach. *Chemical Engineering Science, 58*, 4185–4195.

Riva, M., Compolongo, S., Leva, A. A., Maestrelli, A., & Torreggiani, D. (2005). Structure–property relationships in osmo-air-dehydrated apricot cubes. *Food Research International, 38*, 533–542.

Rodrigues, S., & Fernandes, F. A. N. (2007). Image analysis of osmotically dehydrated fruits: Melons dehydration in a ternary system. *European Food Research and Technology, 225*, 685–691.

Shafafi Zenoozian, M., Devahastin, S., Razavi, M. A., Shahidi, F., & Poreza, H. R. (2008). Use of artificial neural network and image analysis to predict physical properties of osmotically dehydrated pumpkin. *Drying Technology, 26*(1), 132–144.

Shi, J., Pan, Z., McHugh, T. H., & Hirschberg, E. (2009). Effect of infusion method and parameters on solid gain in blueberries. *Food and Bioprocess Technology, 2*, 271–278. doi:10.1007/s11947-008-0116-4.

Spiazzi, E., & Mascheroni, R. (1997). Mass transfer model for osmotic dehydration of fruits and vegetables. I. Development of the simulation model. *Journal of Food Engineering, 34*, 387–410.

Sun, D-W. (ed). (2005). *Emerging Technologies for Food Processing*. London: Academic.

Therdthai, N., & Zhou, W. (2009). Characterization of microwave vacuum drying and hot air drying of mint leaves (*Mentha cordifolia* Opiz ex Fresen). *Journal of Food Engineering, 91*, 482–489.

Tijskens, L. M. M., Schijvens, E. P. H. M., & Biekman, E. S. A. (2001). Modelling the change in colour of broccoli and green beans during blanching. *Innovative Food Science and Emerging Technologies, 2*, 303–313.

Vinod, K. J., & Vikrant, C. (2002). Neural networks approach to modeling food processing operations. In J. M. Irudayaraj (Ed.), *Food processing operations modeling: Design and analysis* (pp. 1–3). New York: Marcel Dekker.